Parallel Integral Equation Based Non-overlapping DDM for Fast Solving Electromagnetic Scattering Problems with Changeable Parts

Zongjing Gu [1], Xunwang Zhao [1], Chang Zhai [1], Zhongchao Lin [1], Yu Zhang [1], and Qi Zhang [2]

[1] Shaanxi Key Laboratory of Large Scale Electromagnetic Computing
Xidian University, Xi'an, Shaanxi 710071, China
xdguzongjing@163.com, xwzhao@mail.xidian.edu.cn, jione92@163.com

[2] Science and Technology on Electromagnetic Compatibility Laboratory
China Ship Development and Design Center, Wuhan 430064, China

Abstract **─** In this paper, a parallel non-overlapping domain decomposition method (DDM) using electric field integral equation (EFIE) is proposed for fast and accurate analysis of electrically large PEC objects with changeable parts in the condition of limited resources. The approach has considered that there are null fields as well as electric current inside a metal object in the original problem, then a novel transmission condition similar to an absorbing boundary is adopted, hence the continuity of electric currents is enhanced and the convergence is further improved in the outer iterative procedure. Moreover, the coupling between different subdomains is calculated in the manner of near field to avoid the storage of the mutual impedance. Some numerical examples are given to demonstrate the efficiency and stability of the proposed method.

Index Terms **─** Domain decomposition method, electrically large, integral equation, transmission condition.

I. INTRODUCTION

In the research field of electromagnetic (EM) scattering, the situation that the local elements located in the overall target rotate or translate while most of the elements remain unchanged is often encountered, for example the gun barrel of a tank rotating or a certain aircraft changing flight posture during formation flying. Generally, in order to study the EM scattering characteristics of the changed model, we have to re-compute the overall target, even though only a small element of the overall target has changed. Obviously, it is extremely time-consumed and wasteful of computing resources for the recalculation of the unchanged parts. It is desirable for computational electromagnetic to provide efficient algorithms for such demands of practical engineering.

Nowadays, Method of Moment (MoM) based on integral equation (IE) is the most accurate numerical methods in the field of computational electromagnetics, which is a numerical method based on Maxwell equation and the boundary conditions of a given problem [1]. However, a huge complex dense matrix will be generated when solving electrically large EM problems, causing that the time taken to solve the matrix equation by using lower/upper (LU) decomposition solver accounts for more than 90% of the total calculation process. More important is that the memory requirement and the computing complexity of the LU solver are in proportion to $O(N^2)$ and $O(N^3)$, respectively, where N is the number of unknowns. Hence, its expensive demands for memory and computing time to solve the matrix equation limit the application of MoM [2]. In order to reduce the memory requirement and computation complexity, the traditional high frequency methods [3, 4] or fast algorithms such as the fast multiple methods [5, 6] are proposed. However, the high frequency methods are at the expense of accuracy, and fast algorithms may confront with slow convergence or even divergence issues in applications involving complex structures [2].

The domain decomposition method (DDM) based on electric field integral equation (EFIE) paves a new way to break through these bottlenecks and has become an effective method to solve electrically large problems [7-10]. In view of this, combining the EFIE with DDM (IE-DDM) makes it possible to solve some problems that we faced. Further, this method provides unprecedented flexibility and convenience for simulating the object with changeable parts, since it stores the unchanged portion matrix after LU factorization in random access memory (RAM) and just needs to re-compute the changed portion of the model during the design process. Finally, the accurate results of each case are obtained through iterative solution and hence the memory requirements and CPU time are reduced greatly. It is should be pointed out that the coupling between different subdomains is obtained using the near field produced by the current to avoid the storage of the mutual impedance [2].

To further improve the ability and efficiency of

Submitted On: October 15, 2018
Accepted On: December 21, 2018

the DDM for simulating scattering performances of electrically large EM objects, one of frequently used and effective ways is to adopt parallel EM algorithm on distributed-memory computers [11-14]. In this case, this paper uses Message Passing Interface (MPI) parallel programming model to accelerate the solution of the EM problems with changeable parts.

This paper is organized as follows. In Section II, the algorithm of the non-overlapping DDM is presented. Section III provides numerical examples to demonstrate the correctness and robustness of the proposed method. Finally, some conclusions are given in Section IV.

II. FORMULATION

A. Domain decomposition strategy

An arbitrarily shaped three-dimensional PEC problem can be modeled with surface integral equations. The scattered electric filed $\boldsymbol{E}^s$ generated by the equivalent electric current $\boldsymbol{J}$ residing on the PEC surface S shown in Fig. 1 can be established firstly [1]:

$$\boldsymbol{E}^s(\boldsymbol{J}(\boldsymbol{r}')) = \eta L(\boldsymbol{J}(\boldsymbol{r}')), \qquad (1)$$

where $\eta = \sqrt{\mu/\varepsilon}$ is the wave impedance in free-space, and $L(\boldsymbol{J}(\boldsymbol{r}))$ is linear operator, which given by:

$$L(\boldsymbol{X}) = -jk\int_S \left[\boldsymbol{X}(\boldsymbol{r}') + \frac{1}{k^2}(\nabla' \cdot \boldsymbol{X}(\boldsymbol{r}'))\nabla \right] G(R)ds', \qquad (2)$$

where G(R) is the Green's function, $R = |\boldsymbol{r} - \boldsymbol{r}'|$ is the distance between the source and the field point. $\boldsymbol{J}(\boldsymbol{r}')$ is the equivalent surface electric current on the PEC surface S and can be expanded in a set of known functions with unknown coefficients a_n^S, which can be expressed as [1, 2]:

$$\boldsymbol{J}(\boldsymbol{r}') = \sum_{n=1}^{N} a_n^{\ S} \boldsymbol{f}_n(\boldsymbol{r}'), \qquad (3)$$

where N is the number of RWG basis functions $\boldsymbol{f}_n(\boldsymbol{r}')$ on surface S [1].

Compared with overlapped DDM [7, 8], the integral equation based non-overlapping domain decomposition method (IE-NDDM) proposed in this paper only adds artificial touching-faces between adjacent subdomains to make each of them closed. In the following, a novel domain decomposition strategy will be introduced. For the sake of clarity, it is considered that a PEC object Ω is divided into three non-overlapping closed subdomains Ω_1, Ω_2 and Ω_3, which is illuminated by incident plane wave $\{E^{inc}, H^{inc}\}$ as shown in Fig. 1. S_m is the exterior boundary except the artificial touching-face $S_{t,m}$ of the subdomains Ω_m. $S_{t,m}$ denotes the artificial touching-face between the subdomain Ω_m and Ω_n except the curve Γ_{mn}. Γ_{mn} is defined as the boundary curve of the artificial touching-face $S_{t,m}$. $\hat{\boldsymbol{n}}_m$ is the outward unit vector of the subdomain Ω_m.

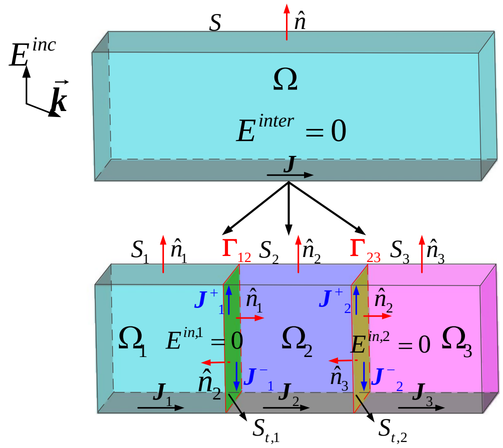

Fig. 1. Decomposition of Ω into three non-overlapping subdomains Ω_1, Ω_2 and Ω_3.

Then, the equation (3) can be rewritten as:

$$\boldsymbol{J}(\boldsymbol{r}') = \sum_{n=1}^{N_1} a_{1,n}^{\ S_1} \boldsymbol{f}_{1,n}(\boldsymbol{r}') + \sum_{n=1}^{N_2} a_{2,n}^{\ S_2} \boldsymbol{f}_{2,n}(\boldsymbol{r}') + \sum_{n=1}^{N_3} a_{3,n}^{\ S_3} \boldsymbol{f}_{3,n}(\boldsymbol{r}'), \qquad (4)$$

where N_m is the number of RWG basis functions on surface S_m. Due to the introduction of artificial touching-face, the current $\boldsymbol{J}_m$ residing on the subdomain m (m=1, 2, 3) can be expressed as:

$$\begin{cases} \boldsymbol{J}_1(\boldsymbol{r}') = \sum_{n=1}^{N_1} a_{1,n}^{\ S_1} \boldsymbol{f}_{1,n}(\boldsymbol{r}') + \sum_{m\in S_{t,1}} a_{1,m}^{\ S_{t,1}} \boldsymbol{f}_{1,m}^{\ S_{t,1}}(\boldsymbol{r}') \\ \boldsymbol{J}_2(\boldsymbol{r}') = \sum_{n=1}^{N_2} a_{2,n}^{\ S_2} \boldsymbol{f}_{2,n}(\boldsymbol{r}') + \sum_{m\in S_{t,1}} a_{2,m}^{\ S_{t,1}} \boldsymbol{f}_{2,m}^{\ S_{t,1}}(\boldsymbol{r}') \\ \qquad + \sum_{m\in S_{t,2}} a_{2,m}^{\ S_{t,2}} \boldsymbol{f}_{2,m}^{\ S_{t,2}}(\boldsymbol{r}') \\ \boldsymbol{J}_3(\boldsymbol{r}') = \sum_{n=1}^{N_3} a_{3,n}^{\ S_3} \boldsymbol{f}_{3,n}(\boldsymbol{r}') + \sum_{m\in S_{t,2}} a_{3,m}^{\ S_{t,2}} \boldsymbol{f}_{3,m}^{\ S_{t,2}}(\boldsymbol{r}') \end{cases}. \qquad (5)$$

Generally, the first order transmission condition is widely used on the artificial touching-faces to ensure the continuity of electric currents, expressed as:

$$\boldsymbol{J}^+{}_m(\boldsymbol{r}') = -\boldsymbol{J}^-{}_m(\boldsymbol{r}'), \quad \boldsymbol{r}' \in S_{t,m}. \qquad (6)$$

In addition, it is well known that there are null electric fields as well as electric currents inside the PEC object as shown in Fig. 1 [1, 2]. With this taken into account, a novel explicit boundary condition is given:

$$a_{1,m}^{\ S_{t,1}} = a_{2,m}^{\ S_{t,1}} = a_{2,m}^{\ S_{t,2}} = a_{3,m}^{\ S_{t,2}}, \quad m \in S_{t,1}, S_{t,2}, \qquad (7)$$

which combines equation (5) and (6) to efficiently solve the PEC problem. In fact, this novel explicit boundary condition can be regarded as an absorbing boundary, which not only enhances the continuity of electric currents across adjacent subdomains, but also ensures the IE-NDDM being equivalent to the original problem (see

Section III.A).

B. Fast solving scattering problems with changeable parts

For explanation purposes, the Galerkin test is adopted to weight linear equation (1) and the following matrix equations is obtained [1, 2]:

$$\begin{bmatrix} \mathbf{Z}_{11} & \mathbf{Z}_{12} & \mathbf{Z}_{13} \\ \mathbf{Z}_{21} & \mathbf{Z}_{22} & \mathbf{Z}_{23} \\ \mathbf{Z}_{31} & \mathbf{Z}_{32} & \mathbf{Z}_{33} \end{bmatrix} \begin{bmatrix} \mathbf{I}_1 \\ \mathbf{I}_2 \\ \mathbf{I}_3 \end{bmatrix} = \begin{bmatrix} \mathbf{V}_1 \\ \mathbf{V}_2 \\ \mathbf{V}_3 \end{bmatrix}, \quad (8)$$

where $\mathbf{Z}_{ij}$ (i=j) is the self-impedance matrix in subdomain Ω_i, $\mathbf{Z}_{ij}$ ($i \neq j$) is the mutual impedance matrix between subdomain Ω_j and Ω_i, $\mathbf{I}_i$ is the unknown current coefficient to be determined and $\mathbf{V}_i$ denotes the given source vector in subdomain Ω_i.

The unknown coefficients will be persistently updated by solving the local model equation until convergence. The number of iteration is initialized being zero (k=0), and the currents in all subdomains are zero ($\mathbf{I}_i(0)=0$ (i=1,2,3)). The user-specified convergence parameter is δ. Setting k=1, 2 …, at k+1th step, the unknown current coefficients can be expressed as:

$$\mathbf{I}_i^{(k+1)} = -\mathbf{Z}_{ii}^{-1}\sum_{j<i}\mathbf{Z}_{ij}\mathbf{I}_j^{(k+1)} - \mathbf{Z}_{ii}^{-1}\sum_{j>i}\mathbf{Z}_{ij}\mathbf{I}_j^{(k)} + \mathbf{Z}_{ii}^{-1}\mathbf{V}_i. \quad (9)$$

The residual error δ_k at kth iteration is used to express the convergence behavior of the iterative method, which is defined as:

$$\delta_k = \frac{\left\| \mathbf{I}_i^{(k)} - \mathbf{I}_i^{(k-1)} \right\|}{\left\| \mathbf{I}_i^{(k)} \right\|}, \quad (i = 1,2,3,). \quad (10)$$

When max (δ_k) ≤ δ at the kth step, the iterative process stops. It is should be pointed out that the mutual impedance in equation (9) is actually unnecessary to be stored and the product $\Delta V_i^{(k+1)}$ of $\mathbf{Z}_{ij}$ and $\mathbf{I}_j^{(k+1)}$ (j<i) or $\Delta V_i^{(k)}$ of $\mathbf{Z}_{ij}$ and $\mathbf{I}_j^{(k)}$ (j>i) can be obtained using the near field produced by the current,

$$\Delta\mathbf{V}_i^{(k)} = \mathbf{Z}_{ij}\mathbf{I}_j^{(k)} = \int_{S^i} \boldsymbol{f}_n(\mathbf{r}')\mathbf{E}_i^{(k)}(\boldsymbol{J})\,\mathrm{d}s, \ (i \neq j), \quad (11)$$

where S^i is the exterior boundary of subdomain Ω_i, and $\mathbf{E}_i^{(k)}$ denotes the nearfield of subdomain Ω_i produced by the rest subdomains at kth step. Hence the memory requirement and CPU time are reduced greatly [16].

In order to describe the process of solving scattering problems with changeable parts using IE-NDDM proposed in this paper, we take the decomposed PEC object with three subdomains shown in Fig. 2 as an example. In this case, compared with Fig. 1, only the posture of subdomain Ω_1 has changed and is named changeable parts. Thus, the self-impedance matrix $\mathbf{Z}_{11}$ in subdomain Ω_1 has changed also [2]. Especially, we have stored the self-impedance matrix of subdomain Ω_2 and Ω_3 after LU factorization in RAM, namely, unchanged portion matrix, when simulating the case shown in Fig. 1. At this time, the computation and factorization of the self-impedance matrix Z_{ii} (i=2, 3) can be avoided to save computing time. Finally, the accurate results can be obtained through iterative solution expressed by equation (9).

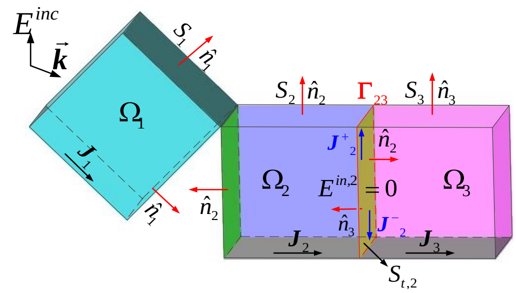

Fig. 2. Notations for domain decomposition with changeable parts.

C. Parallelization implementation on IE-NDDM

In this paper, the parallel IE-NDDM code is implemented through MPI. The flowchart of parallel IE-NDDM solving EM problems with changeable parts is shown in Fig. 3. In order to facilitate the implementation of the algorithm, the changeable parts are divided into one or more subdomains numbered 1, 2…m, during the modeling process.

First step, all parallel processes are used to set up and solve the matrix equation of a single self-domain in turn, until the calculation of all self-domains is finished. The parallel implementation in self-domain mainly involves parallel matrix filling followed by a parallel solution of the dense matrix equation. It is necessary to divide self-domain matrix into matrix blocks and distribute those blocks to different processes for the purpose of load balance. Specifically, a block-cyclic matrix distribution is adopted among processes [2]. In addition, the parallel LU decomposition is utilized as the parallel matrix equation solver for the sake of accuracy [15]. Figure 3 shows this process under the labels computing self-domain matrix.

Second step, the coupling between subdomains is calculated by looping over geometric elements between subdomains, and in consequent, the parallelization of this process could be implemented directly through distributing those geometric elements into different processes uniformly. Figure 3 shows this process under the labels with iterative process.

Third step, once the outer iterative procedure is convergent, the accurate results are obtained through superposition of far-field generated by all subdomains. Figure 3 shows this process under the labels calculating far-field.

If there are one or more changeable subdomains, the changed subdomains need to re-compute according to step 1, this process is shown in Fig. 3 under the labels re-computing changed subdomains, and then, the accurate results of new case are obtained after executing step 2 and step 3.

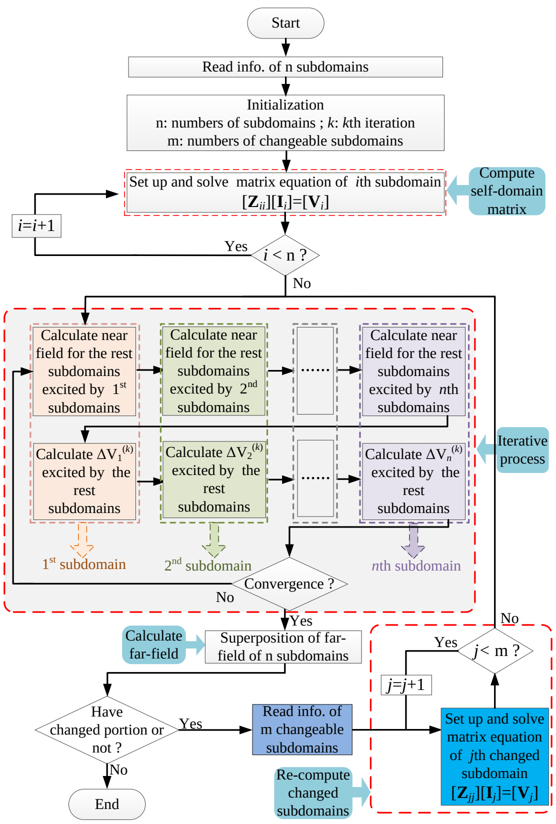

Fig. 3. Parallel framework of IE-NDDM for solving EM problems with m changeable subdomains.

III. NUMERICAL RESULTS

Three EM examples are presented to demonstrate the efficiency and accuracy of the proposed method. The residual error for outer iterative convergence is set to 1.0e–3. The two-dimensional (2D) bistatic radar cross section (RCS) of these classical cases is obtained to present the correctness and robustness of the proposed method. Two computational platforms are used in this paper [16]:

Platform I: A workstation with two six-core 64 bit Intel Xeon E5-2620 2.0 GHz CPUs, 64GB RAM and 6TB disk.

Platform II: High-Performance Computing (HPC) cluster from Xidian University (XD-HPC), which is equipped with 140 compute nodes connected by 56Gbps InfiniBand network, and each node has two 12-core Intel Xeon 2690-v2 2.2GHz CPUs and 64 GB memory.

A. Validation

The first simulation consists of the analysis of a PEC cylinder. The length of the cylinder is 10 m and the diameter is 2m. A *z*-axis polarized plane wave operating at 600MHz impinges along the *x*-axis direction is considered. In this simulation, the model is decomposed into ten subdomains as shown in Fig. 4, where each color represents one subdomain. The bistatic RCS results obtained using in-home MoM code (RWG), FEKO commercial software and IE-NDDM are given, respectively, which are used to validate the accuracy of the method proposed. The simulations are performed using the Platform I aforementioned (24 processes).

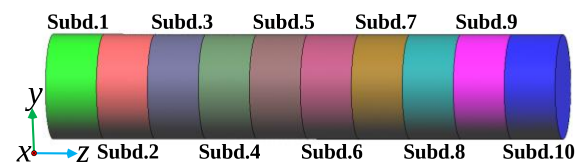

Fig. 4. Model of a cylinder divided into ten subdomains.

Figure 5 shows smooth current distributions, without noticeable discontinuities across subdomain boundaries. Figure 6 shows the RCS comparison for the proposed IE-NDDM, the in-house MoM code and FEKO. It is observed in Fig. 6 that the RCS curves agree well with each other, and the proposed IE-NDDM in this paper is verified and validated. It is observed in Fig. 7 that fast convergence rate has been achieved, which reaches 0.006 at the seventh step in outer-iterative procedure.

The computational resources for solving each subdomain and overall solution are recorded in Table 1. We can observe that the parallel IE-NDDM algorithm leads to almost 68% memory reduction, and the CPU time is greatly reduced.

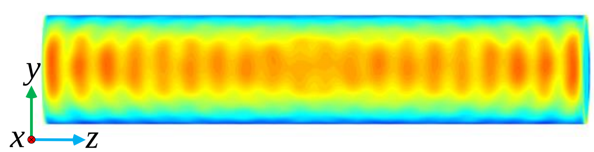

Fig. 5. Surface electric current distribution on the cylinder.

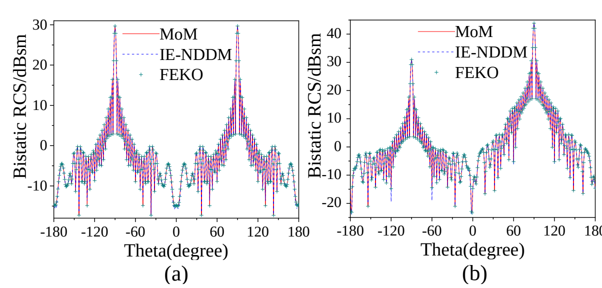

Fig. 6. Bistatic RCS curve of the cylinder: (a) *xoz* plane and (b) *yoz* plane.

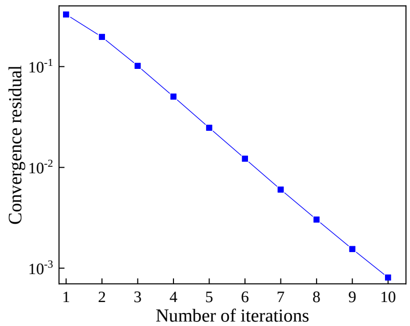

Fig. 7. Convergence curve of IE-NDDM.

Table 1: Computational resources of the cylinder

Method	Unknowns		Storage (GB)	CPU Time (h)
DDM	Subd.1	20112	60.20	8.886
	Subd.2	20052		
	Subd.3	20055		
	Subd.4	20130		
	Subd.5	20109		
	Sudb.6	20106		
	Subd.7	20124		
	Subd.8	20118		
	Subd.9	20097		
	Subd.10	20097		
MoM (RWG)	111636		187.71	12.731
MoM (FEKO)				14.515

B. Scattering from a tank with gun barrel rotating

In this part, the scattering characteristics of a tank with gun barrel rotating are solved to show the advantages of this method in solving local changeable parts problems. The incident plane wave propagates towards head (–*x* axis), and the polarization direction is +*z* axis. The frequency of the plane wave is 1 GHz. Dimension of the tank is 9.5m×3.2m×2.3m, and it is divided into four subdomains, as shown in Fig. 8 with each color representing one subdomain.

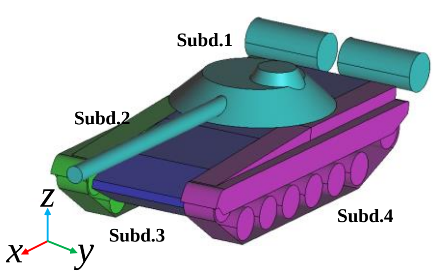

Fig. 8. Model of the tank divided into four subdomains.

The gun barrel rotates along the *z* axis, and the included angle θ_e with x-axis is 0˚, 10˚, 15˚, respectively, as shown in Fig. 9. The simulation is performed on Platform II using 30 compute nodes with each employing 24 processes (720 processes).

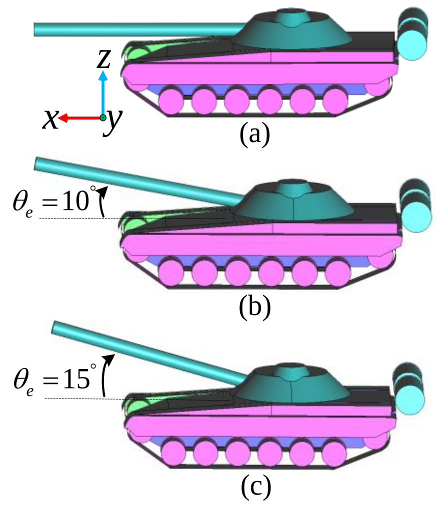

Fig. 9. Model of the tank with gun barrel at different elevation angles: (a) θ_e =0˚, (b) θ_e =10˚, and (c) θ_e =15˚, respectively.

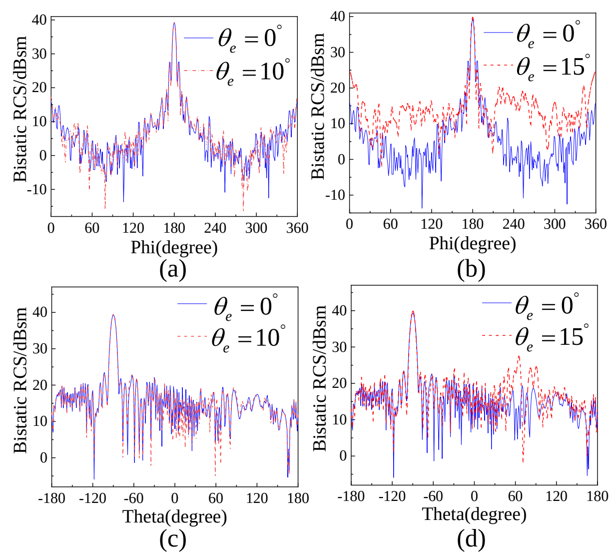

Fig. 10. 2D bistatic RCS curves of the tank with changeable parts: (a) and (b) are *xoy* plane, (c) and (d) are *xoz* plane.

The bistatic RCS results obtained by IE-NDDM are shown in Fig. 10. One can see that the maximum value of RCS remains unchanged basically, when the included angle θ_e with *x* axis is 0˚, 10˚ and 15˚, respectively. Further, RCS values shown in Fig. 10 (a) with $0^\circ \leq \varphi \leq 150^\circ$ and $210^\circ \leq \varphi \leq 360^\circ$, and shown in Fig. 10 (b) with $210^\circ \leq \theta \leq 360^\circ$ has changed greatly when the included angle θ_e is 15˚. The computational resources for solving each subdomain are recorded in Table 2. It can be observed that the method proposed in this paper shows great advantage in solving scattering problems with changeable parts.

Table 2: Computational resources of the tank with gun barrel rotating

Unknowns	Storage (GB)	Posture	CPU Time (h)
Subd.1 108375 Subd.2 120397 Subd.3 150750 Subd.4 120295	945.29	Unchanged parts	2.47
		θ_e=0°	2.26
		θ_e=10°	2.26
		θ_e=15°	2.26
Overall solution 499818	3722.58	--	--

C. Scattering from an aircraft formation

In this example, the scattering characteristics of an aircraft formation with changing flying posture, an electrically large problem, has been solved by parallel IE-NDDM algorithm to further highlight the advantage of the proposed method. The model consists of five aircrafts (one bomber and four fighters), and among which the aircraft numbered I changes its flying posture. As shown in Fig. 11, the aircraft formation is divided into eleven subdomains with each color representing one subdomain, and the distances between aircrafts are given.

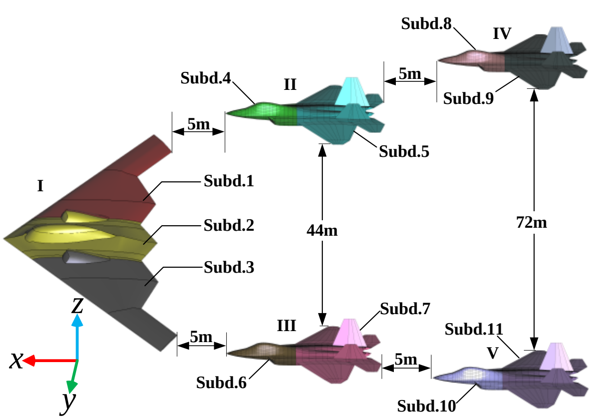

Fig. 11. Model of an aircraft formation.

Particularly, in this simulation, both connected subdomains (e.g., Sub.1 and Sub.2) and unconnected subdomains (e.g., Sub.3 and Sub.4) are included. Due to the fact that the current is discontinuous inherently between unconnected subdomains, hence, there is no need for any transmission conditions between unconnected subdomains, and only the coupling needs to be calculated in the manner of near field.

The included angle θ_e between the flying direction of the aircraft numbered I and x axis is 0°, 15°, 30°, respectively, as shown in Fig. 12. The incident plane wave is toward the nose (-x axis), and is polarized along +z axis, and the operation frequency is 300 MHz.

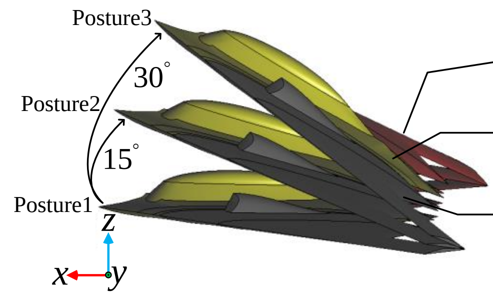

Fig. 12. Model of an aircraft I changing flying posture.

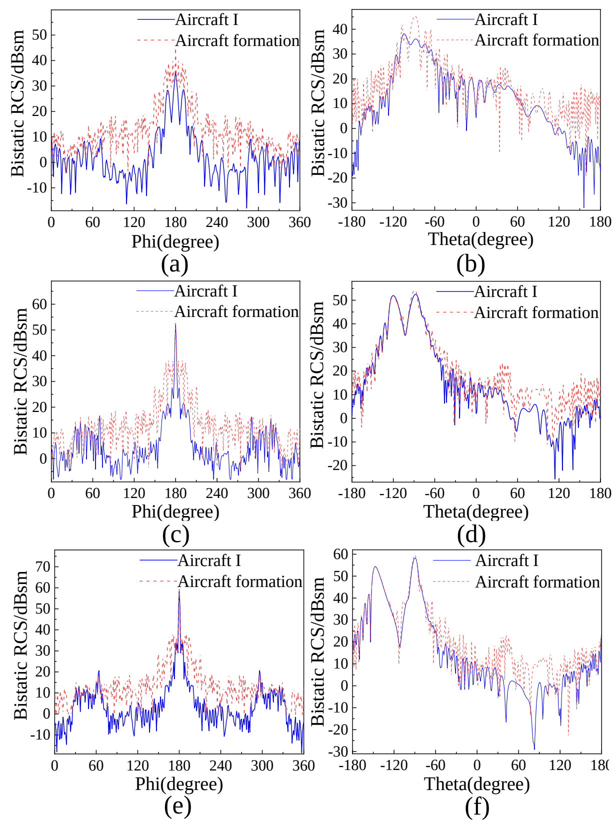

Fig. 13. 2D bistatic RCS curves of the aircraft formation with changeable parts: (a) *xoy* plane with θ_e =0° (posture1), (b) *xoz* plane with θ_e =0° (posture1), (c) *xoy* plane with θ_e =15° (posture2), (d) *xoz* plane with θ_e =15° (posture2), (e) *xoy* plane with θ_e =30° (posture3), and (f) *xoz* plane with θ_e =30° (posture3), respectively.

The simulation is performed on Platform II using 50 compute nodes with each employing 24 processes (1200 processes). The 2D bistatic RCS curves of the aircraft formation obtained by IE-NDDM are shown in Fig. 13. The computational resources for solving each subdomain are accorded in Table 3. As shown in Fig. 13, with the elevation angle θ_e increasing, the contribution of the aircraft I to the bistatic RCS of the entire aircraft formation decreases. And the parallel IE-NDDM saves over 86.8% memory compared with MoM (overall solution).

Table 3: Computational resources of the aircraft formation

Unknowns	Storage (TB)	Posture	CPU Time (h)
Subd.1 100464		Unchanged parts	2.33
Subd.2 125853			
Subd.3 100134			
Subd.4 52152		Posture1	2.9
Subd.5 95379			
Subd.6 52116	1.21		
Subd.7 95382		Posture2	2.9
Subd.8 52122			
Subd.9 95370		Posture3	2.9
Subd.10 52128			
Subd.11 95310			
Overall solution 793182	9.16	--	--

IV. CONCLUSION

An integral equation based on non-overlapping domain decomposition method (IE-NDDM) for the scattering analysis of PEC targets with changeable parts is proposed. A novel explicit transmission condition is applied to enforce the current continuity across adjacent subdomains, which allows the IE-NDDM keep the same level of accuracy than pure techniques such as MoM. Particularly, the coupling between different subdomains is calculated in the manner of near field, which significantly reduces the memory and CPU time. These techniques extend the capability of MoM to solve electrically large problems.

ACKNOWLEDGMENT

This work was supported in part by the National Key Research and Development Program of China under Grant 2017YFB0202102, in part by the National Science Foundation of China under Grant 61301069, in part by the China Postdoctoral Science Foundation funded project under Grant 2017M613068, in part by the National Key Research and Development Program of China under Grant 2016YFE0121600.

REFERENCES

[1] R. F. Harrington, *Field Computations by Moment Methods*. Macmillan, New York, 1968.

[2] Y. Zhang and T. K. Sarkar, *Parallel Solution of Integral Equation Based EM Problems in the Frequency Domain*. Hoboken, NJ: Wiley, 2009.

[3] J. Chen, M. Zhu, M. Wang, S. Li, and X. Li, "A hybrid MoM-PO method combining ACA technique for electromagnetic scattering from target above a rough surface," *ACES Journal*, vol. 29, no. 4, pp. 301-306, 2014.

[4] Y. Kim, H. Kim, K. Bae, J. Park, and N. Myung, "A hybrid UTD-ACGF technique for DOA finding of receiving antenna array on complex environment," *IEEE Trans. Antennas Propag*., vol. 63, no. 11, pp. 5045-5055, 2015.

[5] J. M. Song, C. C. Lu, and W. C. Chew, "Multilevel fast multipole algorithm for electromagnetic scattering by large complex object," *IEEE Trans. Antennas Propag*., vol. 45, no. 10, pp. 1488-1493, 1997.

[6] F. Hu, Z. Nie, and J. Hu, "An efficient parallel multilevel fast multipole algorithm for large-scale scattering problems," *ACES Journal*, vol. 25, no. 4, pp. 381-387, 2010.

[7] K. Han, Z. Nie, and Y. Wang, "A simply constructed overlapped domain decomposition method for solving large scattering problems," *Electromagnetics*, vol. 36, no. 7, pp. 470-484, 2016. DOI: 10.1080/02726343.2016.1220908.

[8] W. Li, W. Hong, and H. Zhou, "Integral equation-based overlapped domain decomposition method for the analysis of electromagnetic scattering of 3D conducting objects," *Microwave & Optical Technology Letters*, vol. 49, no. 5, pp. 1225-1230, 2007. DOI: 10.1002/mop.22479.

[9] W. Li, H. Zhou, J. Hu, et al., "An ODDM-based solution to CFIE with impedance boundary condition," *IEEE Antennas & Wireless Propagation Letters*, vol. 10, no. 9, pp. 1197-1200, 2011. DOI: 10.1109/LAWP.2011.2172969.

[10] Z. Peng, R. Hiptmair, Y. Shao, et al., "Domain decomposition preconditioning for surface integral equations in solving challenging electromagnetic scattering problems," *IEEE Transactions on Antennas & Propagation*, vol. 64, no. 1, pp. 210-223, 2015. DOI: 10.1109/TAP.2015.2500908.

[11] L. Gurel and O. Ergul, "Hierarchical parallelization of the multilevel fast multipole algorithm (MLFMA)," *Proc. IEEE*, vol. 101, no. 2, pp. 332-341, Feb. 2013.

[12] B. Michiels, J. Fostier, I. Bogaert, and D. De Zutter, "Full-wave simulations of electromagnetic scattering problems with billions of unknowns," *IEEE Trans. Antennas Propag*., vol. 63, no. 2, pp. 796-799, 2015.

[13] X. M. Pan, and X. Q. Sheng, "A sophisticated parallel MLFMA for scattering by extremely large targets," *IEEE Antennas Propag. Mag*., vol. 50, no. 3, pp. 129-138, June, 2008.

[14] X. M. Pan, W. C. Pi, M. L. Yang, Z. Peng, and X. Q. Sheng, "Solving problems with over one billion unknowns by the MLFMA," *IEEE Trans. Antennas Propag*., vol. 60, no. 5, pp. 2571-2574, 2012.

[15] X. Zhao, Y. Chen, H. Zhang, Y. Zhang, and T. K. Sarkar, "A new decomposition solver for complex electromagnetic problems," *IEEE Antennas Propag*. Mag., vol. 59, no. 3, pp. 131-140, 2017.
[16] A. Tzoulis and T. F. Eibert, "Efficient electromagnetic near-field computation by the multilevel fast multipole method employing mixed near-field/far-field translations," *IEEE Antennas and Wireless Propagation Letters*, vol. 4, pp. 449-452, 2005.

Zongjing Gu received the B.S. degree from ShanDong Normal University, JiNan, China, in 2013, and is currently working toward the Ph.D. degree at Xidian University. His current research interests is computational electromagnetic.

Xunwang Zhao received the B.S., and Ph.D. degrees from Xidian University, Xi'an, China, in 2004, and 2008, respectively. He joined Xidian University as a Faculty Member in 2008. As Principal Investigator, he is doing or has completed some projects including project of NSFC.